

# A Special Feeder for Diffraction Pattern Analysis of Dry Powders

Kurt Leschonski, Stephan Röthele, Ulrich Menzel\*

(Received: 25 May 1984)

## Abstract

Numerous unit operations in particle technology require that dry powders are fed into a system with as little fluctuation as possible in flow rate and velocity and that the powder is dispersed in flowing air. A feeding and dispersing system has been developed

which allows mass throughputs between 0.1 and 20 kg/h. It has been used as a feeder unit for dry particle size analysis from diffraction patterns.

## 1 Introduction

In the continuous dispersion of dry particulate solids, especially in the size range below 20  $\mu\text{m}$ , it is of decisive importance to overcome the cohesive forces between individual particles. This paper describes the development of a feeding and dispersing system which entrains particles in a gas stream and deagglomerates them by shear forces in a high velocity turbulent flow and by impact against solid surfaces. The degree of dispersion so achieved was determined from the analysis of the diffraction pattern of a laser light beam produced by the particles in a free jet. The measurements were primarily performed with the Leeds and Northrup Microtrac.

The feeder described here has been an object of studies for some time using the basic principle for the delivery of predetermined feed rates to air classifiers with minimum fluctuation; the generation of particle streams for the study of two phase flow systems; the feeding of powders in powder coating applications and as a feeder for dry particle size analysis. The major difference between the feeder described here and conventional aerosol generators lies in its capacity to deliver mass flow rates from 0.1 kg/h to approximately 20 kg/h.

Proper dispersion is difficult to achieve, since fine particles cling together due to adhesion forces which often surpass by several orders of magnitude the weight of the particle. The smaller the particles are, the bigger the dispersion problems will be.

Possible solutions to the problem of dispersing agglomerates into individual particles depend on the knowledge and understanding of adhesion forces acting between particle surfaces. *H. Rumpf* [1] suggested in 1958 a classification of adhesion forces as van der Waals, electrostatic and magnetic forces, as well as forces due to liquid or solid bridges between the particles. Van der Waals, electrostatic forces and forces due to liquid bridges are the ones to be taken into consideration when discussing means to disperse fine powders.

A reasonable description of the physics of adhesion would exceed the scope of this paper. Those interested in further information

should refer to *H. Krupp* [2] published in 1967 on "particle adhesion, theory and experiment" and further papers published by *H. Rumpf* and *E. Turba* [3], *F. Löffler* [4], *W. Pietsch* [5], *W. Herrmann* [6], *K. Borho* [7] and *H. Schubert* [8]. According to these authors, van der Waals forces and forces due to liquid bridges are predominant in the dispersion of powders, electrostatic adhesion is of no importance in the agglomerate. Electrostatic forces may, however, be generated as soon as the dispersion, that is the separation of solid particle surfaces, has taken place. Electrostatic charging can change the behaviour of the particles in such a way that almost immediate reagglomeration of the particles and adhesion of particles to the walls of the feeder and other units occurs [7]. Dispersion is, therefore, not only synonymous with deagglomeration but also with its stabilisation.

*A. Zahradnicek* [9, 10] has investigated the dispersion in gases, of quartz and limestone particles with size between 0.5 and 10  $\mu\text{m}$ . His findings are, until now, the only ones available to describe quantitatively the systematic dispersion of powders in gases. The experimental results obtained by *A. Zahradnicek* not only have fundamental significance but can also be applied to the dispersion of powders in a feeder as developed here. Methods to disperse powders in gases have also been used in aerosol generators. The following main principles have been applied:

- a) the acceleration of particles in an ejector,
- b) the flow of particles and gas through a jet with a narrow gap,
- c) the flow of particles and gas through a bent tube,
- d) the impingement of high speed jets onto the surface of a powder.

These techniques show the basic principles for dispersion of powders in gases, high rates of shear flow and wall contacts. *Zahradnicek* showed, quantitatively, that only a combination of both effects yields the desired dispersion in a particle size range between 2 and 10  $\mu\text{m}$ , shear flow alone is not sufficient. It may be concluded from his results that not only air velocities of the order of 100 m/s and above should be chosen, but the particles to be dispersed should also suffer an impact.

Good dispersion is only of value, however, as long as it is not neutralized by secondary, immediate agglomeration. The particles should, therefore, be separated from each other as far as possible after dispersion, in order to avoid secondary adhesion. Farreaching adhesion forces causing secondary agglomeration

\* Prof. Dr.-Ing. K. Leschonski, Dipl.-Ing. S. Röthele, Dipl.-Ing. U. Menzel, Institut für Mechanische Verfahrenstechnik der TU Clausthal, Leibnizstr. 15, D-3392 Clausthal-Zellerfeld (Federal Republic of Germany).

are mainly the electrostatic ones. In all cases of practical application, where secondary agglomeration might occur, one should therefore neutralize surplus charges as obtained during dispersion. This can be achieved either by ionising or by moisturising the gas surrounding the particles.

The production of suitable positive or negative ions may be achieved using a corona discharge as suggested by *K. T. Whitby* [11]. The flux of ions produced depends on the diameter and spacing of the electrodes, gas pressure and the voltage used between the two electrodes. Due to the fast recombination of the ions, the mixing of the ionized gas with the charged aerosol should take place as closely as possible to the zone of production of the ions. Discharging an aerosol with a radioactive source has been investigated by *B. Y. H. Liu* and *D. Y. H. Pui* [12]. Both methods, however, are applicable only in processes where solids concentration and solids flow rate are low. This is due to the fact that the permissible activity of a radioactive source limits the ion production and, furthermore, the process of electrostatic discharge occupies a finite time.

In most cases of practical application, therefore, very little is done to prevent reagglomeration. However, especially on dry days in the winter, the addition of water vapour may improve the dispersion considerably. Care should be taken to adjust and maintain the moisture content of the air to a value between 50 and 60% relative humidity. Dispersion may be enhanced and reagglomeration can be reduced in certain cases, also, by adding a suitable dry dispersing agent such as a colloidal silicic acid to the feed material. In the latter case the influence of van der Waals forces may be greatly reduced.

In many cases, however, one further problem is encountered when dispersing the feed material. In order to overcome adhesion forces acting between small particles, high gas velocities and impacts must be used for dispersion. The stresses produced in the agglomerates may be big enough to break the particles themselves and dispersion may therefore lead to an undesired comminution of the feed material. Irregularly shaped particles may lose corners or edges, this leading to the production of new fine material. It is therefore always necessary to pay attention to the comminution of the feed material caused by the dispersing unit. One should also remember that wall-particle interactions may not only break the particle but, with hard materials, may also cause wear. This aspect should, therefore, be taken into account when selecting materials of construction for such a feeder [13].

## 2 Experimental Arrangement

Figure 1 shows a plan view of the experimental arrangement, with the various components of the dispersing feeder identified. They consist of a feed hopper and vibratory chute, a rotary table with a U-shaped groove near its periphery, a scraper, a compacting roller and an ejector into whose inlet a rotating brush introduces the powder, followed finally by a cascade impactor which acts as a dispersing system. The particles leave the dispersion stage in the ejector air stream. At a point downstream, a laser beam intercepts the solids laden free jet, with the volume of intersection forming the measuring zone. Figure 2 shows the various substages of the two major processes, feeding and dispersion.

### 2.1 Feeding

The U-shaped groove on the rotating table is overfilled with the particulate feed by means of a vibratory feeder. A certain degree of sample splitting is simultaneously achieved since only a

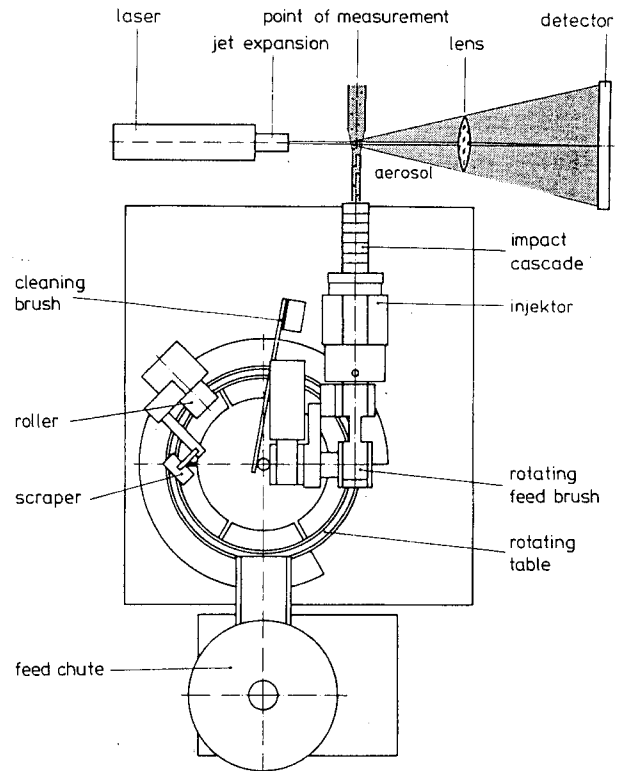


Fig. 1: Components of the dispersing feeder.

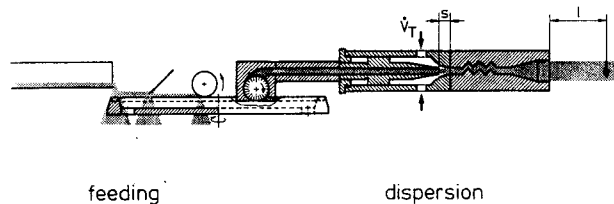


Fig. 2: Schematic representation of the steps necessary for the production of a free jet, uniformly loaded with dispersed particulates.

portion of the feed enters the groove. The material remaining in the groove then passes first under a plough scraper, whose height above the groove is adjustable, and then under a fixed roller which compacts it. The homogeneity of material achieved by this procedure ensures that the rotating brush, which carries material into the suction zone of the ejector, does so at a constant rate without pulsation or fluctuation. If the sample is free flowing and shows no tendency to agglomerate, the rotating brush may be dispensed with and the powder sucked directly into the ejector from the groove. When cohesive materials are handled, however, this procedure leads to cracks in the compacted powder stream appearing along the sides of the groove and powder entering the ejector in a discontinuous fashion, leading to strong pulsations.

### 2.2 Dispersion

Four factors ensure that dispersion begins as soon as the material enters the ejector:

First the particles are accelerated due to the increasing admixture of air which is induced by the primary, or driving, volume flow rate of air,  $\dot{V}_T$ . This enters the ejector through an annular space,

driven by a pressure,  $p_T$ , and induces a secondary volume flow rate of air,  $V_S$ , in the central or suction tube of the ejector. The driving air can be controlled both by varying,  $p_T$ , and the space,  $s$ , between the exit of the central tube and the mixing zone of the ejector.

Secondly the annular space through which the driving air enters the ejector is contoured, allowing the creation of a high shear zone.

Thirdly the particle-particle and particle-wall interactions during the entire pneumatic transport of the particles through the ejector.

Finally total dispersion is achieved by the incorporation of an impact cascade at the end of the ejector mixing zone. The solids thus dispersed emerge as a free jet and are intercepted by a laser beam at a distance,  $l$ , on the ejector axis measured from their point of emergence.

Feed or mass flow rates are controlled by varying either the speed of the rotating table or the dimensions of the groove. Feed rates are dependent, also, on the bulk properties of the sample and whether or not the rotating feed brush has to be used. With free flowing materials sucked directly from the groove, feed rates between 0.1 and 20 kg/h have been achieved but incorporation of the brush reduces the upper limit.

**2.3 Definition of the Degree of Dispersion**

In order to assess the accuracy of the particle size distribution obtained using this procedure, it is necessary to determine the degree of dispersion achieved. A parameter, similar to one suggested by A. Zahradnicek [9], has been defined which consists of the ratio between two moments of the size distribution. The  $k^{\text{th}}$  moment of the  $q_r$  density distribution is defined by:

$$M_{k,r} = \int_{x_{\min}}^{x_{\max}} x^k q_r(x) dx \tag{1}$$

The degree of dispersion was described by the moment related to the specific surface of the particles,  $M_{-1,3}$ . It has been determined from both dry analysis,  $M_{-1,3}$ , and from an analysis performed on a completely dispersed suspension of the same sample in a liquid,  $M_{-1,3}$ . The degree of dispersion was then calculated from:

$$\beta_{-1,3} = M_{-1,3} / M_{-1,3}^* \sim S_V \tag{2}$$

If dispersion in the dry state is complete,  $\beta_{-1,3}$  attains the value of one, with values between nought and one indicating the presence of undispersed agglomerates.

For a completely unambiguous assessment of the dry powder analysis, a second parameter can be defined which relates to the relative volume of the particles in the zone of measurement. This is defined as

$$\beta_{3,3} = M_{3,3}^* / M_{3,3} \sim V \tag{3}$$

$\beta_{3,3}$ , through its relationship with particle volume, gives an indication of the comparability of the dry analysis to the reference analysis with respect to the transport concentration. This is of particular importance in particle size analysis performed on solids carried in free jets, since large particles have velocities which differ from those of the fine particles which leads to a false estimate of the relative quantities of different sizes in the zone of measurement.

The reference moment is made the numerator in the definition of  $\beta_{3,3}$  in order to adhere to the convention that full dispersion is indicated by the appropriate parameter achieving a value of unity while lesser degrees of dispersion are represented by values between 0 and 1.

**2.4 Determination of the Reference Distributions**

The reference moments  $M_{-1,3}^*$  and  $M_{3,3}^*$  were determined after the samples were dispersed in an ultrasonic bath using a liquid containing a dispersing agent. Figure 3 shows the size distributions which were used in testing the feed, feedrate control and dispersion units. As seen in the figure, the upper sizes are 10, 20 and 30  $\mu\text{m}$  respectively and have varying proportions, by weight, below 5  $\mu\text{m}$ . The finest distribution contains 65% below 5  $\mu\text{m}$ , while the most widely tested distribution, K 200, contains 40%. The  $x_{50,3}$  values are 4, 6, 15 and 35  $\mu\text{m}$ , with the coarsest distribution being used only to check the range of mass flow rates which could be obtained. The  $M_{-1,3}^*$  values are also indicated on the figure and are used later in the determination of  $\beta_{-1,3}$ .

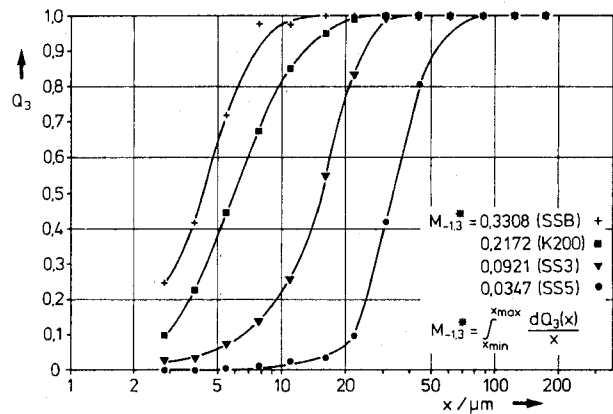


Fig. 3: Size distributions examined.

**3 Experimental Results**

**3.1 Feeding**

Figure 4 shows the feed transport characteristics of the different substages. The fluctuations in mass flow rate were determined photometrically and plotted against time, using an  $x-t$  recorder. A comparison of the traces show the different characteristics of the stages. The measurements are first made on the overfilled groove, starting six seconds after feeding begins. Fluctuations in mass flow rate amount to  $\pm 43.8\%$  in this section, with a mean rate of 7.7 kg/h being achieved. After the plough scraper, the fluctuations are reduced to  $\pm 15.7\%$ , with the rate dropping to 4.5 kg/h. Finally, the roller reduces both values further to  $\pm 4\%$  and 3.8 kg/h, respectively. These latter fluctuations are due to the material in the sides of the groove being picked up unevenly, and could be reduced further to  $\pm 2.5\%$ , by the introduction of the rotating feed brush. They are low enough to allow the use of the dispersing feeder as the generator of a solids laden free jet used for the purpose of determining the particle size distributions of the solids by diffraction pattern analysis [15].

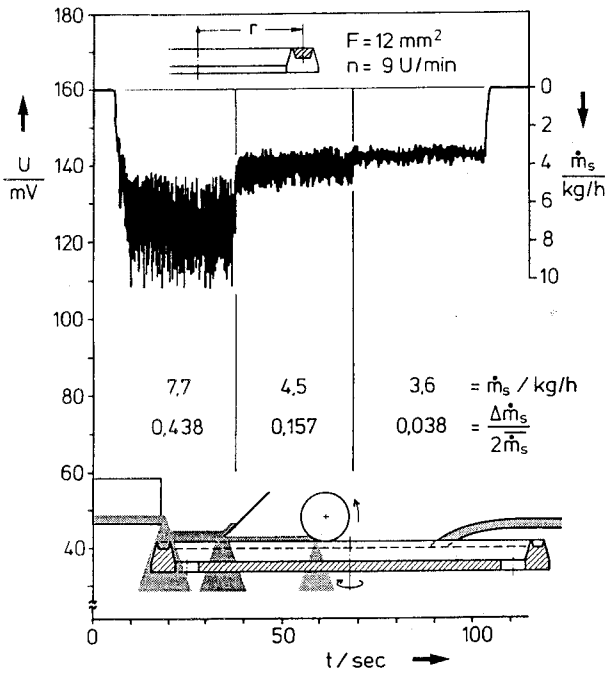


Fig. 4: Mass flow and fluctuation of the substages.

3.2 Dispersion

Figure 5 shows, in three dimensions, the effects of both throat spacing  $s$  and driving pressure  $p_T$  on the degree of dispersion achieved.

In the experiments described above, the shear force field due to the velocity gradient in the nozzle area of the ejector was the major dispersion mechanism. The degree of dispersion is seen to increase with decreasing  $s$  until a maximum is observed at  $s = 0.5$  mm. If  $s$  is decreased further, a pulsation of the induced air flow occurs followed by a complete cessation of transport as the driving air is completely throttled. Regardless of  $s$ , the degree of dispersion varies somewhat unpredictably with  $p_T$  in the range  $1.5 < p_T < 2.5$  bar, with a maximum of  $\beta_{-1,3} = 0.76$  being achieved at  $p_T = 2.5$  bar and  $s = 0.5$  mm.

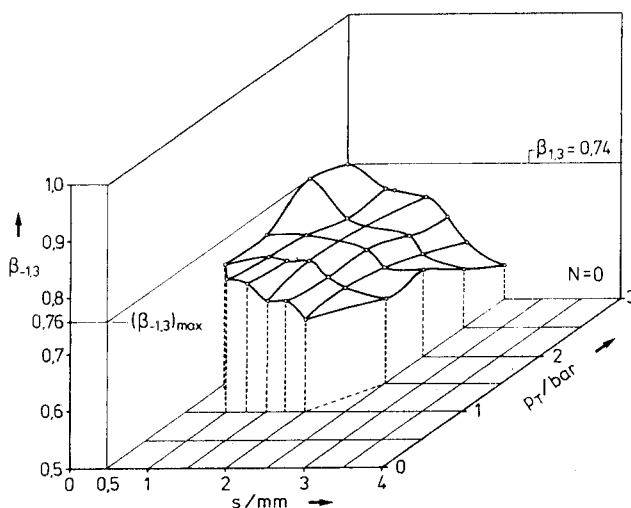


Fig. 5: The degree of dispersion  $\beta_{-1,3}$  as a function of nozzle spacing  $s$ , and driving pressure  $p_T$  (feed: SS3).

When impact surfaces are introduced after the mixing zone of the ejector, the degree of dispersion is noticeably enhanced. Figure 6 shows how  $\beta_{-1,3}$  is affected by the number of such impact stages.  $\beta_{-1,3}$  is increased to  $>0.9$  when the impact cascade has three stages, while a further increase in the number of stages leads to a slight reduction in its value. The impact surfaces of the cascade were inclined at  $60^\circ$  to the principal flow. Angles of  $30^\circ$  were also tested with no improvement being observed in the degree of dispersion. The remaining experiments were performed using an impact cascade with three stages at inclined  $60^\circ$  to the direction of flow.

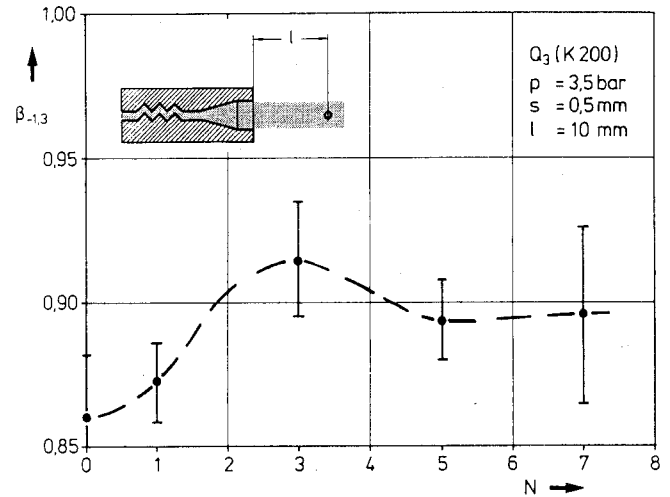


Fig. 6: Influence of the number of impact stages  $N$  of the degree of dispersion  $\beta_{-1,3}$ .

The results shown in Figure 5 were based on measurements made immediately after the solids bearing free jet emerged from the expander stage of the ejector. The decision to place the measuring point there was based on an assumption that dispersion was complete by the times this point is reached. The degree of dispersion, indicated by the  $\beta_{-1,3}$  values, indicates the influence of particle velocity, which is dependent on particle size, on the result. This causes the size analyses to appear coarser than they really are, [14], which is probably caused by the large particles emerging from the expander at lower velocities than the small ones and so spending a disproportionately long time in the measuring zone. If, however, the measuring zone is moved further down the axis, then the expanding free jet will loose velocity and slow down the small particles, due to drag, to a greater extent than the large ones which possess more inertia. This effect should, therefore, act to reestablish a more representative presence of all the size in the measuring zone.

This is confirmed by the behaviour of  $\beta_{-1,3}$ , shown in Figure 7, which reaches a maxima for measurements made at 30 – 40 mm from the ejector exit with no impact stages, as well as with one and three impact stages. The greatest degree of dispersion is again seen to occur with three impact stages and the optimum distance of 40 mm, when  $\beta_{-1,3}$  reaches a value of 0.97.

Figure 8 shows the effect discussed above on the particle size distribution. Size distributions determined from measurements made near the ejector outlet appear coarser than the reference, distributions whilst when the measuring zone is 40 mm away from the outlet the result shows good agreement with the reference analysis.

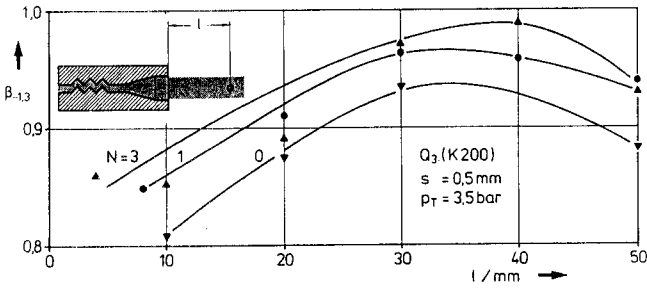


Fig. 7: Maximum values of the degree of dispersion as a function of impact stages  $N$ , and position of measuring zone  $l$ .

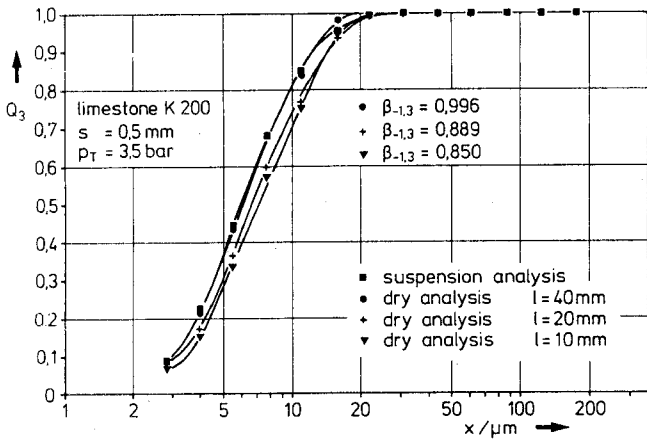


Fig. 8: Particle size distributions (feed: K200).

Figure 9 confirms this result for the coarser distribution, SS 3, containing particles up to  $40 \mu\text{m}$  in size with a median size of  $15 \mu\text{m}$ . The effect is not quite as noticeable as before. This is because the task of dispersion is facilitated because of the reduction in the superfine particles present in SS 3, whilst K 200 has a narrow distribution which tends to mitigate the distorting effects of the transport concentration.

Having established the optimum value for  $l$  and  $N$  the influence on the degree of dispersion of nozzle spacing,  $s$ , and driving pressure,  $p_T$ , were re-examined. The results are shown in Figure 10.

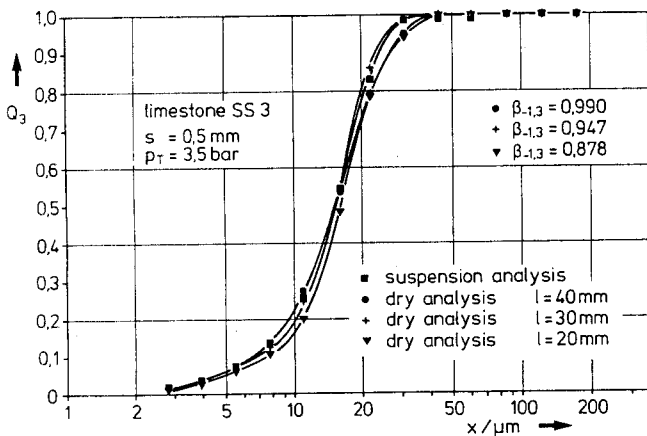


Fig. 9: Particle size distributions (feed: SS3).

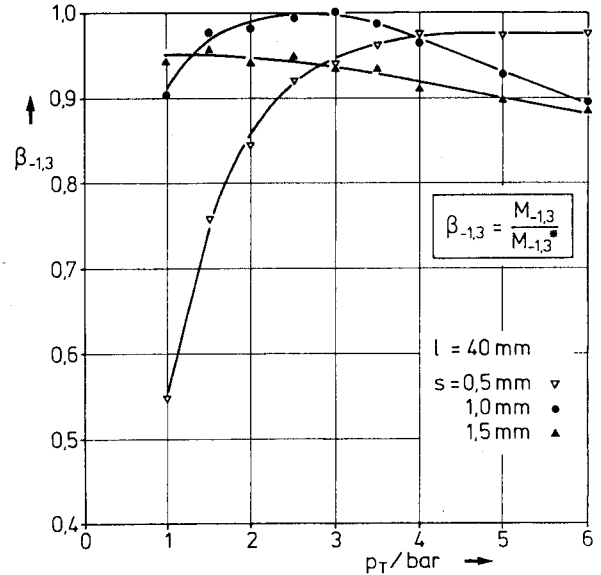


Fig. 10: Variation of degree of dispersion with ejector driving pressure  $p_T$  and nozzle spacing  $s$  ( $N = 3$ ).

It is observed that the optimum nozzle spacing,  $s = 0.5 \text{ mm}$ , as previously found, gives a degree of dispersion which increases monotonically with  $p_T$  until it reaches a value of 0.97, at about  $p_T = 4 \text{ bar}$ , after which it remains constant. For  $s = 1.0 \text{ mm}$ ,  $\beta_{-1,3}$  increases with  $p_T$  until when  $p_T$  equals 2.5 bar it reaches unity and decreases thereafter. When  $s = 1.5 \text{ mm}$  the degree of dispersion is fairly high, even at low pressure, but it never reaches unity and decreases slowly with increasing pressure.

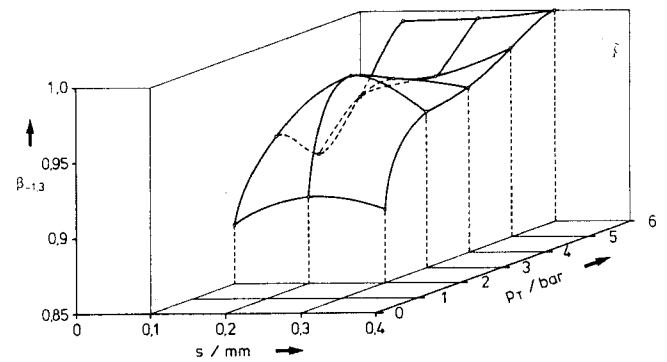


Fig. 11: The degree of dispersion  $\beta_{-1,3}$  as a function of driving pressure  $p_T$  and nozzle spacing  $s$  when a rotating feed brush is used ( $N = 3$ ,  $l = 30 \text{ mm}$ ).

When the rotating feed brush is used, the picture again changes and the optimum nozzle spacing is reduced. Figure 11 shows, three dimensionally, the variation of  $\beta_{-1,3}$  with nozzle spacing,  $s$ , and driving pressure,  $p_T$ . With increasing pressure, a first maximum is reached for all nozzle spacings at 3 bar, with the largest value,  $\beta_{-1,3} = 0.98$ , being obtained for a value of  $s$  of 0.2 mm. When the pressure is increased further, the degree of dispersion first decreases and then increases again and becomes unity for a nozzle spacing of 0.3 mm, and the maximum driving pressure, 6 bar, which was available for these experiments.

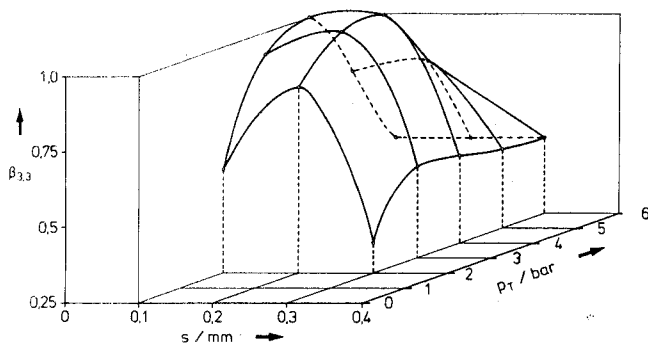


Fig. 12: The degree of concentration  $\beta_{3,3}$  as a function of driving pressure  $p_T$  and nozzle spacing  $s$  when a rotating feed brush is used ( $N = 3$ ,  $l = 30$  mm).

In order to unambiguously determine the operating conditions, the second parameter indicating dispersion, the degree of concentration,  $\beta_{3,3}$ , was then determined. Figure 12 shows, three dimensionally, the variation of  $\beta_{3,3}$  with  $s$  and  $p_T$ . Quite clearly  $\beta_{3,3}$  has a maximum at  $s = 0.2$  mm and  $p_T = 3.5$  bar. This set of conditions, therefore, is the best for use in particle size analysis, and allows a reproducible comparison of the dry analyses performed using free solids/gas jets with those performed with the particles dispersed in a liquid in the conventional way.

#### 4 Conclusion

The investigation of a dispersing feeder has demonstrated that it is suitable for use in obtaining particle size distributions by means of diffraction pattern analysis, even with very fine powders, and that these analyses are comparable with reference analyses performed on liquid suspensions. In order to obtain reliable results it is necessary to condition and handle the powder correctly in the feeding stage, and to deagglomerate it using both flow and impact forces in the dispersing stage.

#### 5 Symbols and Abbreviations

$l$	distance of laser beam to ejector orifice
$M_{k,r}$	$k$ -th moment of the $q_r$ -distribution
$\dot{m}_s$	particle mass flow
$N$	number of impact stages
$p_T$	propellant pressure
$q_r$	density distribution
$Q_r$	cumulative distribution
$s$	ejector crevice width
$S_v$	specific surface area

$t$	time
$U$	voltage
$V$	volume
$\dot{V}_T$	propellant jet stream
$\dot{V}_S$	induced jet stream
$x$	particle size
$x_{\min}$	minimum particle size
$x_{\max}$	maximum particle size
$x_{50}$	mean particle size
$\beta_{-1,3}$	degree of dispersion
$\beta_{3,3}$	degree of concentration

#### 6 References

- [1] *H. Rumpf*: Grundlagen und Methoden des Granulierens. Chem. Ing. Tech. 30 (1958) 144 – 158.
- [2] *H. Krupp*: Advances in Colloid and Interface Science. Elsevier, Amsterdam 1967, Vol. 1.
- [3] *H. Rumpf, E. Turba*: Über die Zugfestigkeit von Agglomeraten bei verschiedenen Bindemechanismen. Ber. Dt. Keram. Ges. 41(1964) 78 – 84.
- [4] *F. Löffler*: Untersuchung der Haftkräfte zwischen Feststoffteilchen und Faseroberflächen. Staub-Reinhaltung Luft 26 (1964) 274 – 280.
- [5] *W. Pietsch*: Das Agglomerationsverhalten feiner Teilchen. Staub-Reinhaltung Luft 27 (1967) 20 – 33.
- [6] *W. Herrmann*: Die Adsorption von Wasserdampf in Schwespat-Preßlingen und ihr Einfluß auf deren Festigkeit. Dissertation Universität Karlsruhe, 1971.
- [7] *K. Borho*: Zum Problem des Dispergierens von Stäuben. Staub-Reinhaltung Luft 33 (1973) 317 – 319.
- [8] *H. Schubert*: Untersuchungen zur Ermittlung von Kapillardruck und Zugfestigkeit von feuchten Haufwerken aus körnigen Stoffen. Dissertation Universität Karlsruhe, 1972.
- [9] *A. Zahradnick*: Untersuchung zur Dispergierung von Quarz- und Kalksteinfraktionen im Korngrößenbereich 0.5 – 10  $\mu\text{m}$  in strömenden Gasen. Dissertation Universität Karlsruhe, 1976.
- [10] *A. Zahradnick*: Methoden zur Aerosolherstellung aus vorgegebenen Feststoffhaufwerken. Staub-Reinhaltung Luft 33(1975) 226 – 231.
- [11] *K. T. Whitby*: Generator For Producing High Concentrations of Small Ions. Rev. Sci. Instr. 32 (1961) 1351 – 1355.
- [12] *B. Y. H. Liu, D. Y. H. Pui*: Electrical Neutralization of Aerosols. Aerosol Science 5 (1974) 465 – 472.
- [13] *K. Leschonski*: Classification of Particles in Gases. IFPRI-Report, Clausthal 1981.
- [14] *J. Raasch, H. Umhauer*: Grundsätzliche Überlegungen zur Messung der Verteilungen von Partikelgröße und Partikelgeschwindigkeit disperser Phasen in Strömungen. Chem. Ing. Tech. 49 (1977) 931 – 941.
- [15] *M. Heuer*: Verfahren zur Berechnung der Partikelgrößenverteilung aus Beugungsspektren. Vortrag auf der 3. Fachtagung "Granulometrie 1983", Dresden.